

Characterization of $\text{Ni}_{57}\text{Zr}_{20}\text{Ti}_{20}\text{Sn}_3$ amorphous powders obtained by mechanical alloying

Hsin-Ming Wu^a, Shih-Sheng Hung^b, Pee-Yew Lee^{c,*}

^a Department of Materials Engineering, Tatung University, Taipei 104, Taiwan

^b Department of Materials Science and Engineering, I-Shou University, Kaohsiung 840, Taiwan

^c Institute of Materials Engineering, National Taiwan Ocean University, Keelung 202, Taiwan

Available online 9 October 2006

Abstract

This study examined the amorphization behavior and thermal stability of mechanically alloyed $\text{Ni}_{57}\text{Zr}_{20}\text{Ti}_{20}\text{Sn}_3$ powders synthesized by high-energy ball milling. Complete amorphization is feasible after 5 h of milling. The thermal stability of the $\text{Ni}_{57}\text{Zr}_{20}\text{Ti}_{20}\text{Sn}_3$ amorphous powders was investigated by differential thermal analysis. As the results demonstrated, the temperature interval of the supercooled liquid region defined by the difference between glass-transition temperature and crystallization temperature is 96 K for $\text{Ni}_{57}\text{Zr}_{20}\text{Ti}_{20}\text{Sn}_3$. The glass-transition and crystallization temperatures of mechanically alloyed samples are different from those reported in the literature for samples prepared by melt spinning techniques. The different thermal stability is believed to be due to the introduction of impurities into the ball-milled samples during mechanical alloying process. The glass transition behavior in the $\text{Ni}_{57}\text{Zr}_{20}\text{Ti}_{20}\text{Sn}_3$ is found to be a kinetically modified thermodynamic phase transformation process. © 2006 Elsevier B.V. All rights reserved.

Keywords: Ni-based alloys; Amorphous phase; Mechanical alloying; Supercooled liquid region; Glass transition

1. Introduction

Recently, new metallic amorphous alloys with a wide supercooled liquid region exceeding 20 K have been prepared in a number of Ni-based alloy systems, such as $\text{Ni}_{76}\text{M}_5\text{P}_{19}$ ($\text{M} = \text{Ti}, \text{Zr}, \text{Hf}$ or Nb), $\text{Ni}_{75-x}\text{Nb}_5\text{M}_x\text{P}_{20-y}\text{B}_y$ ($\text{M} = \text{Cr}, \text{Mo}$), and Ni-Ti-Zr-(Al,Sn) [1–3]. The supercooled liquid region is defined by the temperature range, $\Delta T = T_x - T_g$, between the glass transition temperature (T_g) and crystallization temperature (T_x). The increase in ΔT means that the stability of the supercooled liquid state against crystallization increases and, therefore, enables the formation of bulk amorphous alloys by conventional casting techniques at a low cooling rates ranging from 1.5 to 100 K/s. Indeed, the bulk amorphous $\text{Ni}_{75-x}\text{Nb}_5\text{M}_x\text{P}_{20-y}\text{B}_y$ alloys with diameter up to 1 mm have been produced by Wang et al. [2].

It is well known that both high reduced glass transition temperature T_g/T_m and large supercooled liquid region ΔT are essential for the formation of bulk amorphous alloys by rapid solidification. However, this also restricts bulk glass

formation to near-eutectic compositions where supercooling can be realized without nucleation of crystalline phases. An alternative way to prepare amorphous alloy is via solid-state amorphization reaction (SSAR processes) [4]. SSAR is a low temperature process; therefore, it circumvents the limitations of conventional alloying and allows forming amorphous samples for compositions which cannot be amorphized by casting techniques. The techniques to synthesize amorphous alloys via SSAR include hydrogenation, multilayer interdiffusion, and mechanical alloying (MA). As previous investigations demonstrated, amorphization by mechanical alloying has been observed for a variety of binary and ternary alloy systems [5–7]. The product material of mechanical alloying is in powder form and is suitable for compaction and densification in many shapes. It is therefore very interesting to investigate the feasibility of preparing Ni-based amorphous alloys by mechanical alloying. In this paper, we report on the formation and thermal stability of mechanically alloyed $\text{Ni}_{57}\text{Zr}_{20}\text{Ti}_{20}\text{Sn}_3$ powders prepared by high-energy ball milling.

2. Experimental procedure

Elemental powders of Ni (99.9%, <300 mesh), Zr (99.9%, <100 mesh), Ti (99.9%, <325 mesh), Sn (99.9%, <100 mesh), were weighed to yield the desired

* Corresponding author. Tel.: +886 2 24622192; fax: +886 2 24625324.
E-mail address: pylee@mail.ntou.edu.tw (P.-Y. Lee).

composition $\text{Ni}_{57}\text{Zr}_{20}\text{Ti}_{20}\text{Sn}_3$, and then canned into an SKH 9 high speed steel vial together with Cr steel balls in an argon-filled glove box, where a SPEX 8016 shaker ball mill was employed for MA. The overall mechanical alloying process was persisted for 5 h and was interrupted every 15 min during the first hour and every 30 min afterwards. At each interruption, a suitable quantity of the powders was extracted to examine the progress of amorphization reaction. Techniques used to examine the status of amorphization included X-ray diffraction analysis and differential scanning calorimetry (DSC). The X-ray analysis was performed using a SIEMENS D-5000 diffractometer with a monochromatic $\text{Cu K}\alpha$ radiation. The thermal stability of the as-milled powders was investigated using a Dupont 2000 differential scanning calorimeter, where the sample was heated from room temperature to 700 °C under a purified argon atmosphere at constant heating rates of 10, 20, 30 and 40 K/min.

3. Results and discussion

Fig. 1 shows the X-ray diffraction patterns of the starting and as-milled $\text{Ni}_{57}\text{Zr}_{20}\text{Ti}_{20}\text{Sn}_3$ powders as a function of milling time. The top curve shows the X-ray diffraction pattern of a mixture of pure crystalline Zr, Ni, Ti and Sn peaks. After 2 h of ball milling, the peak intensities of Ti and Sn decreased rapidly, indicating a preferential alloying of these two elements with either Ni or Zr. With further ball milling up to 5 h, all the crystalline peaks have disappeared; only a broad diffraction peak is left, indicating that amorphization is complete within the resolution of X-ray diffraction.

The thermal stability of $\text{Ni}_{57}\text{Zr}_{20}\text{Ti}_{20}\text{Sn}_3$ amorphous powders was investigated by differential scanning calorimetry.

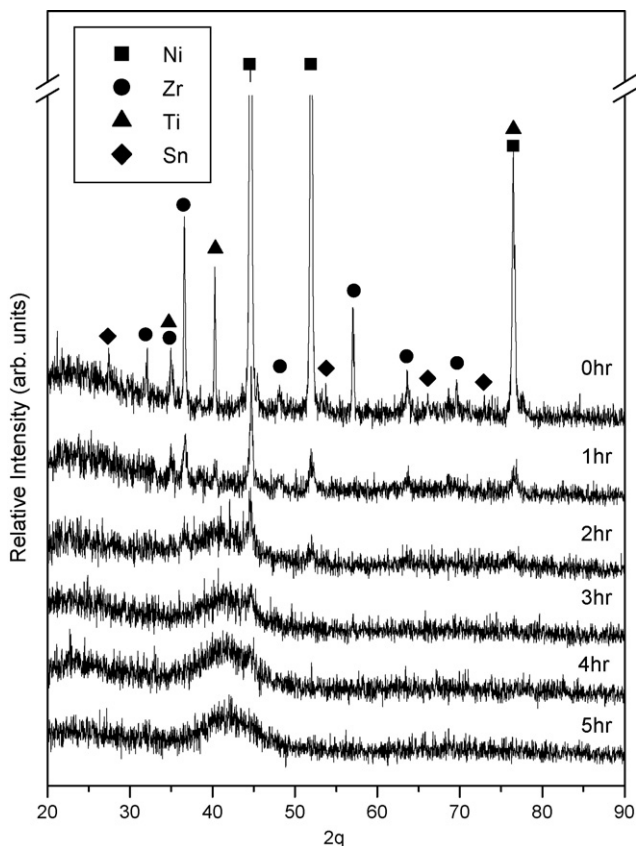


Fig. 1. X-ray diffraction patterns of mechanically alloyed $\text{Ni}_{57}\text{Zr}_{20}\text{Ti}_{20}\text{Sn}_3$ powders as a function of milling time.

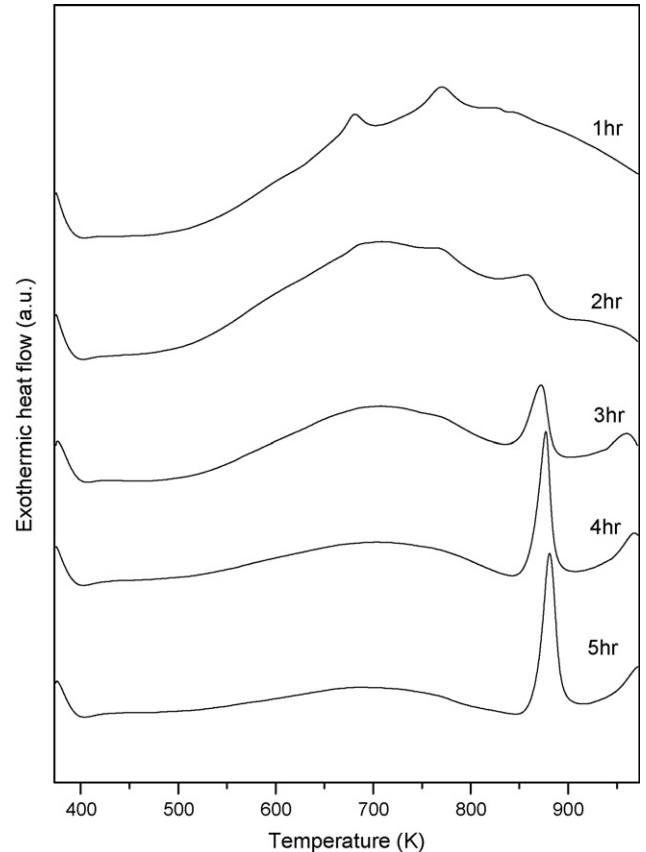


Fig. 2. DSC trace of amorphous $\text{Ni}_{57}\text{Zr}_{20}\text{Ti}_{20}\text{Sn}_3$ powder obtained at a heating rate of 40 K/min.

Fig. 2 shows the DSC curve of the amorphous ball-milled $\text{Ni}_{57}\text{Zr}_{20}\text{Ti}_{20}\text{Sn}_3$ alloys. It can be seen that the amorphous powders exhibit an endothermic heat event due to the glass transition followed by a sharp exothermic peak indicating the transformation from a supercooled liquid state to crystalline phase. The glass transition and crystallization temperatures were defined as the onset temperatures of the endothermic and exothermic DSC events, respectively. The glass transition temperature (T_g) and the crystallization temperature (T_x) are 771 and 867 K, respectively. The supercooled liquid region ΔT is 96 K. For melt-spun $\text{Ni}_{57}\text{Zr}_{20}\text{Ti}_{16}\text{Si}_2\text{Sn}_3$ amorphous alloys, Lee et al. [6] have reported that T_g , T_x and ΔT measured at a heating rate of 30 K/min are 815, 878 and 63 K, respectively. MA is a high-energy ball milling process involving the collision of fine powders with milling balls and vial. The oxygen and iron contents in mechanically alloyed powders are always more than 1 at.% due to the large surface area of the fine particles and iron contamination from the milling tools. Seidel et al. [8] have investigated the effect of oxygen and iron on the thermal properties of mechanically alloyed and rapidly quenched Zr–Al–Cu–Ni and Zr–Ti–Cu–Ni alloys. The mechanically alloyed $\text{Zr}_{65}\text{Al}_{7.5}\text{Cu}_{17.5}\text{Ni}_{10}$ powders with different iron and oxygen contents exhibited lower T_x and ΔT values than those of quenched samples, while fluctuating glass transition temperatures were noticed. Their results also indicated that the influence of oxygen impurities is more significant than that of

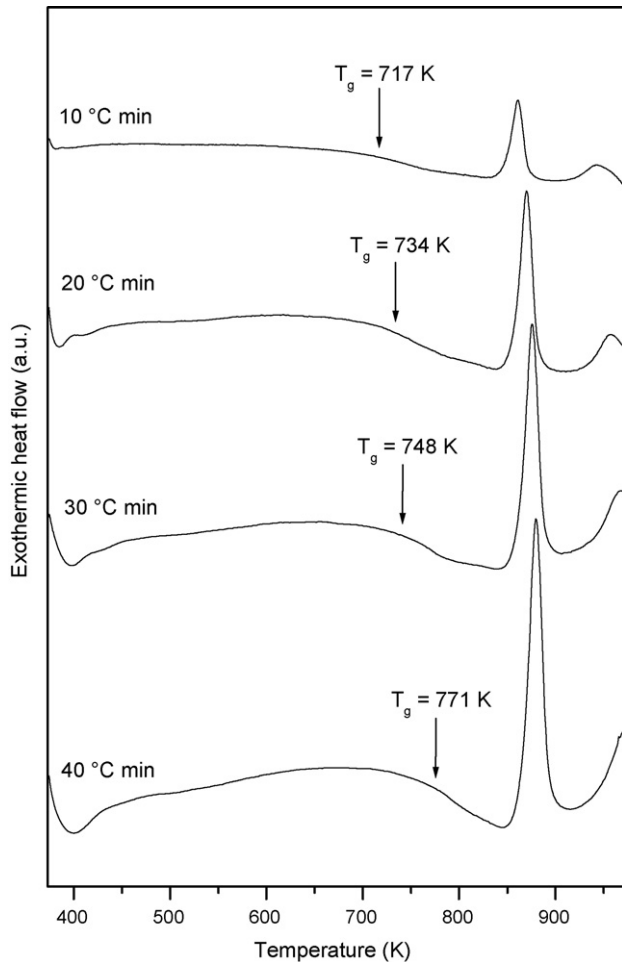


Fig. 3. Dependence of glass transition temperature (T_g) with respect to heating rate (Φ) for the amorphous $\text{Ni}_{57}\text{Zr}_{20}\text{Ti}_{20}\text{Sn}_3$ powders.

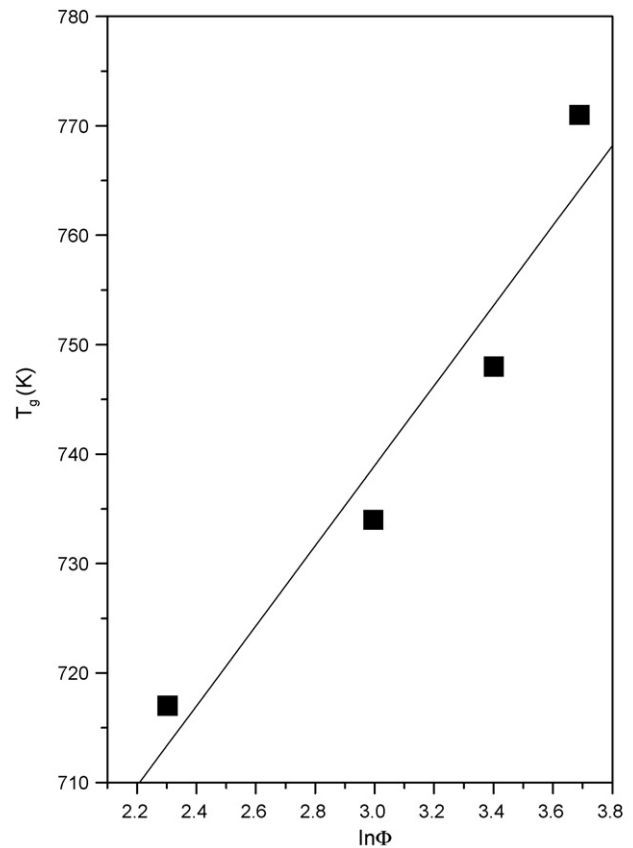


Fig. 4. The linear relationship between T_g and $\ln \Phi$.

iron contaminations. Very recently, Lin et al. [9] have studied the thermal stability of Zr–Ti–Al–Cu–Ni amorphous alloys prepared by mechanical alloying. The thermal stability of some mechanically alloyed Zr–Ti–Al–Cu–Ni amorphous alloys shows similar behavior as the results reported in Ref. [8] for mechanically alloyed $\text{Zr}_{65}\text{Al}_{7.5}\text{Cu}_{17.5}\text{Ni}_{10}$ amorphous alloys. However, the T_g , T_x and ΔT of several mechanically alloyed samples were higher than those of squeeze cast specimens [10]. Though the effects of contamination were not investigated in the current study, the impurity contents were presumably responsible for the different thermal stability of mechanically alloyed powders and melt-spun specimens.

Neither a glass transition nor a supercooled liquid region are observed for the melt spun $\text{Ni}_{77-x}\text{Zr}_x\text{Ti}_{23}$ ($x=10, 20, 30, 40$) amorphous alloys [3]. In contrast to this, previous work [3] and the present study all indicate that the addition of Sn could induce the occurrence of a supercooled liquid region in melt-spun $\text{Ni}_{57}\text{Zr}_{20}\text{Ti}_{16}\text{Si}_2\text{Sn}_3$ and mechanically alloyed $\text{Ni}_{57}\text{Zr}_{20}\text{Ti}_{20}\text{Sn}_3$ amorphous alloys. Inoue et al. [11] suggested that large atomic size ratios, attractive bonding nature between the main constituent elements, together with the difficulty of the redistribution of these elements for crystallization are dominant factors for the increase in glass-forming ability and the appearance of a

wide supercooled liquid region. For the $\text{Ni}_{57}\text{Zr}_{20}\text{Ti}_{20}\text{Sn}_3$ composition, the differences in the atomic sizes of Ni and the other elements exceed 11% (the atomic radii of Ni, Zr, Ti and Sn are 0.125, 0.160, 0.145 and 0.162 nm, respectively). It is believed that these atomic size differences lead to the highly dense random packed structure in the amorphous phase, which enables the achievement of a large liquid/solid interfacial energy and makes the redistribution of atoms on a large range scale difficult. In addition, the Ni–Zr, Ni–Ti and Ni–Sn atomic pairs also have a highly attractive bonding nature as a result of their large negative heat of mixing ΔH_m [12]. The above-mentioned characteristics of the alloy suppress nucleation and growth of crystalline phases in the supercooled liquid phase, and thus lead to a large glass forming ability and a high thermal stability in the $\text{Ni}_{57}\text{Zr}_{20}\text{Ti}_{20}\text{Sn}_3$ alloy.

Finally, the glass transition behavior of the $\text{Ni}_{57}\text{Zr}_{20}\text{Ti}_{20}\text{Sn}_3$ was investigated by DSC scans using various heating rates. Fig. 3 shows the DSC scans obtained at the different heating rates of 10, 20, 30 and 40 K/min, respectively. Both T_g and T_x are shifted to higher temperature with increasing heating rate, revealing that not only crystallization but also the glass transition temperature of the amorphous powders depend on the heating rate during continuous heating. This phenomenon implies that the glass transition behaves in a marked kinetic manner. The dependence of T_g on the heating rate (Φ) follows the Lasocka's relationship [13]: $T_g = A + B \ln \Phi$, where A and B are constants for a given glass composition.

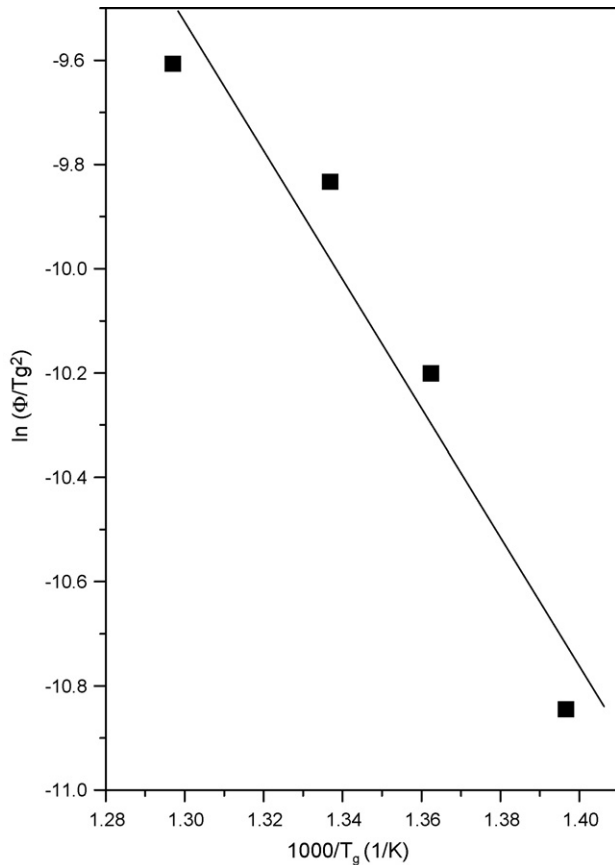


Fig. 5. Kissinger's plot of amorphous Ni₅₇Zr₂₀Ti₂₀Sn₃ powder.

Table 1
 T_g , T_x , ΔT , E_g , A , and B for amorphous Ni₅₇Zr₂₀Ti₂₀Sn₃ powders

T_g (K)	771
T_x (K)	867
ΔT (K)	96
E_g (eV)	1.07
A	629.2
B	36.5

T_g , T_x , and ΔT are measured at a heating rate of 40 K/min. $T_g = A + B \ln \Phi$.

Fig. 4 shows the linear relationship between T_g and $\ln \Phi$. Furthermore, the effective activation energy (E_g) for the glass transition can be determined by the Kissinger's peak shift method [14]. The linear relationship between $\ln(\Phi/T_g^2)$ and $1/T_g$ for the Ni₅₇Zr₂₀Ti₂₀Sn₃ alloy is shown in Fig. 5, where E_g was deduced from the slope of the curve. Table 1 summarizes the values of A , B , and E_g . Based on our experimental results

shown above, the glass transition process of the amorphous Ni₅₇Zr₂₀Ti₂₀Sn₃ powders can be regarded as a kinetically modified thermodynamic phase transformation process.

4. Conclusions

We have studied the amorphization behavior of Ni₅₇Zr₂₀Ti₂₀Sn₃ alloy powders synthesized by mechanical alloying. Complete amorphization is feasible after ball milling for 5 h. The amorphous powders were found to exhibit a wide supercooled liquid region of 96 K before crystallization. This demonstrates the potential of mechanical alloying as a versatile method for the formation of Ni₅₇Zr₂₀Ti₂₀Sn₃ amorphous alloys with wide supercooled liquid region. The glass transition temperature T_g and the crystallization temperature T_x of mechanically alloyed samples are different from those of specimens prepared by melt-spinning. It is suspected that the different thermal properties arise from the introduction of impurities during the mechanical alloying process. A kinetically modified thermodynamic phase transformation process was observed for the glass transition behavior in the Ni₅₇Zr₂₀Ti₂₀Sn₃ amorphous powders.

Acknowledgement

The authors are grateful for the financial support of this work by the National Science Council of Republic of China under Grant No. NSC 90-2216-E-019-002.

References

- [1] R. Akatsuka, T. Zhang, H. Koshiba, A. Inoue, Mater. Trans. JIM 40 (1999) 258–261.
- [2] X.M. Wang, I. Yoshii, A. Inoue, Y.-H. Kim, I.-B. Kim, Mater. Trans. JIM 40 (1999) 1130–1136.
- [3] T.G. Park, S. Yi, D.H. Kim, Scripta Mater. 43 (2000) 109–114.
- [4] W.L. Johnson, Prog. Mater. Sci. 30 (1986) 81–134.
- [5] C. Politis, W.L. Johnson, J. Appl. Phys. 60 (1986) 1147–1151.
- [6] P.Y. Lee, C.C. Koch, J. Mater. Sci. 23 (1988) 2837–2845.
- [7] P.Y. Lee, J.L. Yang, C.K. Lin, H.M. Lin, Metall. Mater. Trans. A 28 (1997) 1429–1435.
- [8] M. Seidel, J. Eckert, L. Schultz, Mater. Sci. Forum 235–238 (1997) 29–34.
- [9] C.K. Lin, S.W. Liu, P.Y. Lee, Metall. Mater. Trans. A 32A (2001) 1777–1786.
- [10] T. Zhang, A. Inoue, Mater. Trans. JIM 39 (1998) 857–862.
- [11] A. Inoue, T. Zhang, T. Masumoto, J. Non-Cryst. Solids 156–158 (1993) 473–480.
- [12] A.R. Miedema, P.F. Dechatel, F.R. de Boer, Physica B 100 (1980) 1–28.
- [13] M. Lasocka, Mater. Sci. Eng. 23 (1976) 173–177.
- [14] H.E. Kissinger, Anal. Chem. 29 (1957) 1702–1706.